International Journal of Nanoelectronics and Materials
Volume 15 (Special Issue) December 2022 [1-12]

Niobium Pentoxide Nanostructures Fabricated by the Fundamental Q-Switched Nd:YAG PLD under Vacuum Conditions

Suhair R. Shafeeq[1], Evan T. Salim[2,*], and Mohammed Jalal AbdulRazzaq[1]

[1]Laser and Optoelectronic Engineering, University of Technology-Iraq,
10066 Baghdad, Iraq
[2]Applied Science Department, University of Technology-Iraq,
10066 Baghdad, Iraq

ABSTRACT

In this paper, we outline the successful preparation of a nanostructured Nb_2O_5 thin film by utilizing Q-switched Nd:YAG pulsed laser in a vacuum environment. The deposition was performed with the fundamental wavelength, 350 ºC as substrate temperature and laser energy of 657 mJ. The film optical, structural, topographical, and morphological properties were investigated by the UV-Visible spectrophotometer, photoluminescence, XRD analyses, AFM, and FE-SEM. The elemental compositions were also tested by EDX analyses. The estimated indirect band gap value (confirmed by PL) agreed with many reported works and studies. It was also well suited for various applications. The data extracted from XRD profile provided well-defined Polycrystalline peaks with the orthorhombic phase (T-Nb_2O_5) as the predominant plane. Monoclinic (H-Nb_2O_5), commonly formed at very high route temperatures, was interestingly formed by PLD technique at a substrate temperature of only 350 ºC. The obtained structures were characterized without any post- annealing treatment.

Keywords: Nanostructured, orthorhombic, PLD. quantum dot

1. INTRODUCTION

Niobium is a member of 5-transition elements family, provides various states of oxidation that are formed in Niobium oxides such as NbO, NbO_2, Nb_2O_3 and Nb_2O_5[1-3]. Nb_2O_5 is the most attractive niobium- oxide configuration in the field of research due to its unique physiochemical properties[4, 5]. Nb_2O_5 possesses the features of a wide n-semiconductor band gap, air stability, water-insolubility, high thermodynamic stability and corrosion resistance that qualify it for various industrial and medical applications[6-9]. Nb_2O_5 is majorly formed in polymorphs. There have been 15 reported phases up to now, with pseudohexagonal assigned as (TT-Nb_2O_5), orthorhombic indicated by (T-Nb_2O_5) and monoclinic symbolized with (H-Nb_2O_5) are the most prominent and have widely been incorporated in a wide range of applications[6, 10]. Since 1940s, interests have been increased about Nb_2O_5 behavior, however further studies about Nb_2O_5 thin films and nanostructures are still required [11-13]. Different routes have been utilized to synthesize and prepare Nb_2O_5 thin films such as sol-gel technique [14, 15], anodization method[16, 17], hydrothermal technique[18, 19], RF magnetron sputtering[20, 21], atomic layer deposition [22, 23], and pulsed laser deposition technique[24, 25]. Preparing Nb_2O_5 by PLD technique has insufficiently been studied; hence further investigations are required to obtain high quality films that can be incorporated in current and future applications. Pulsed laser deposition technique (PLD) provides several advantages as compared with other synthesize routes. The directed confined plume is produced with the same stoichiometry of the target material is one of these advantages. When the material is deposited with the same target stoichiometry, a thin film with high quality can be produced. Other benefits of PLD technique include the low cost and the deposition process can be performed in a short time. In addition, a wide range of materials can be deposited by PLD without reactant agents or chemical additives [26-29]. As the particle size

* evan.t.salim@uotechnology.edu.iq, & evan_tarq@yahoo.com

modification is one of the most significant features in nanotechnology, different particle size can be easily obtained via PLD technique due to the fact that the deposition parameters are controllable. These parameters include the selected laser wavelength, the laser fluence, pulse duration, and the number of laser pulses. Other conditions such as target-substrate distance, substrate temperature, background compositions and pressure are all controllable and impact on films growth. In pulsed laser deposition method, no precursors are required as in sol-gel, spray and pyrolysis techniques. Furthermore, in electrochemical deposition technique, a long time is required in Nb_2O_5 formation process and pollutants can be produced through the electroplating mechanism [26, 30]. In pulsed laser deposition, no pollutants can be observed due to the deposition process occurs inside a vacuum chamber or within a mixed background gas.

Decreasing the size of the nano particle is one of the desirable features in nanotechnology. As the particle size lies within the range of 2 to 10 nm, the particle is called "Quantum dot" that provides unique features due to its surface-to-volume ratio increased that it exhibits the quantum confinement phenomena [31, 32]. In pulsed laser deposition technique, quantum dots can be synthesized by using very short laser pulse duration (in fs range), short wavelengths such as excimer lasers, and other parameters such as background gas that provides collisions with plasma plume species and fragmentation process to smaller size can be occurred as the collision exhibits transferring the kinetic energy [33-38].

In 1999, the electrochemical and electrochromic properties of Niobium Oxide thin films deposited on ITO glass substrate in oxygen background mixture (O_3/O_2) were investigated by Z. Fu et al.[39] with the third harmonic wavelength of Nd:YAG laser (λ=335 nm) that was employed for the deposition process. The substrate temperature was (200) °C. The obtained XRD diffraction pattern revealed that Nb_2O_5 thin film was amorphous and it was polycrystalline when annealed to 500 °C with pseudohexagonal (TT-Nb_2O_5) phase structure obtained. In 2011, a vertical alignment of Nb_2O_5 bundles nanocrystals synthesized by Ghosh et al.[40]. KrF laser (λ =248 nm) with laser pulse energy of (300) mJ were selected as the deposition parameters. The deposition process was performed in oxygen background that was varied to study its effect on the obtained Nb_2O_5 nanostructures. The background gas and pressure were changed to study their impact on the produced films' morphologies and photophysical properties. A high number of laser pulses used that was also varied to investigate the number of pulses impact. The number of laser shots were (2, 10, 20, 60, and 300) k, respectively. The XRD results demonstrated the orthorhombic (T-Nb_2O_5) structure after the prepared films were annealed to 500 °C. The obtained results were applied as photoanodes and showed an improvement in the performance of the device. Physical properties of the annealed Nb_2O_5 thin films obtained in a vacuum condition and deposited by Q-switched Nd:YAG laser were studied by Fakhri et al.[13]. The deposition parameters including Nd:YAG laser wavelength (λ= 1064 nm), 250ºC as the substrate temperature, and 250 laser shots were employed. The deposited Nb_2O_5 thin films were annealed at 400, 500, and 600 °C, respectively. The results of XRD analyses showed the monoclinic structure (H-Nb_2O_5) as the predominant phase.

In this work, we aim to study the structural, optical,topographical, and morphological behavior of the Niobium pentoxide thin film deposited by Q-switched pulsed Nd:YAG laser with specific selected parameters. In addition, the elemental compositions of the obtained Nb_2O_5 thin film were analyzed by EDX spectroscopy. The deposition process was performed in vacuum without any background gas. The prepared sample was tested as-deposited without any annealing or post-treatment.

2. EXPERIMENTAL SET-UP

The tools including the p-type 111 silicon wafers substrates were cleaned and sterilized for removing any contaminants, fingerprints or other atmospheric impurities including dust particles. For this purpose, an ultrasonic device filled with a suitable amount of deionized water mixed with some drops of ethanol (analytical grade C_2H_5OH) was used. Fifteen minutes later, the substrates and the other required tools were carefully dried. Nb_2O_5 in the form of powder with a weight of (3g) was pressed under 12 tons of pressure by hydraulic compressor for (2 minutes) into a pellet. The hydraulic compressor's mold was rinsed with hydrochloric acid (HCl) and deionized water then polished by employing MPD dual speed grinder-polisher device producing a circular disk-like shape target pellet, shown in Figure 1, with a diameter of (2.5 cm) and a height of (0.5 cm).

Figure 1. Nb_2O_5 target used for deposition process.

Q-switched Nd:YAG pulsed laser with the fundamental wavelength was utilized for the deposition process. The selected parameters, summarized in Table 1, were carefully chosen and totally different than the previous works to provide a further investigation of Nb_2O_5 thin film behavior.

Table 1. The selected parameters for preparing Nb_2O_5 thin film

Laser energy	657 mJ
Number of pulses	200
Laser shots frequency	3 Hz
Focal length	12 cm
Target-to-substrate distance	10 cm
Substrate temperature	350 ºC
Target material	Nb_2O_5 Merck (Kenilworth, NJ) with ultra-purity (99.99%), pressure in a 2.5 cm diameter and 0.5 cm height a disk-like shape.

After the primary conditions including the chamber pressure and the substrate temperature were fixed at the selected values, the deposition process was accurately performed. The target was regularly rotated by a raster fixed with PLD system. The obtained film was characterized by the double beam (Shimadzu, 1800) UV-Visible spectrophotometer to investigate the absorbance and the optical band gap value. The absorption coefficient as a function of a wavelength range was calculated by[41-45]:

$$\alpha = \frac{2.303\ A}{t} \quad (cm^{-1}) \tag{1}$$

where (α) is the absorption coefficient, (A) is the absorbance and (t) is the obtained thin film thickness. The incident photon energy was calculated by [46-48]:

$$E_{g=\frac{1240}{\lambda}} \quad (eV) \tag{2}$$

The band gap of the prepared film was estimated by Tauc equation[49-52]:

$$(\alpha h\nu) = B(h\nu - Eg)^{0.5} \tag{3}$$

Where (h) is Planck's constant, (v) is the incident photon frequency, (B) is a constant parameter of the band tailing, (r) is a constant with different values relying on the estimated material transitions. Photoluminescence was performed by (Firmware version: 131024 with serial No. FS-1401004) for further indication of the band gap obtained value. The prepared thin film's thickness was measured by Fizeau interference[37] fringes by using the following equation [53-55]:

$$t = \frac{316.4\ \Delta x}{x} \quad (nm) \tag{4}$$

Where (x) represents the bright fringe width and (Δx) is the two adjacent fringes spacing. Structural analyses were investigated by the (Shimadzu, 6000 cu-kα) XRD scanning device. The crystallites' size of the formed crystal planes were calculated by Scherrer's equation[49, 56-58]:

$$D = \frac{K\lambda}{\beta * \cos(\theta)} \quad (nm) \tag{5}$$

Where (D) is the crystallite size, (K) is constant value (0.94), λ is the X-ray exciting wavelength (1.54 Å), (β) is the full widths at half maxima, and (θ) is the half position angle inclined between the incident and the scattered wavelength. The dislocation densities were measured by [49, 59, 60]:

$$\delta = \frac{1}{D^2} (line.m^{-2}) \tag{6}$$

(δ) is defined as the dislocation density and (D) is the crystallite size (nm). The microstrain of were measured by Wilson formula [49, 61, 62]:

$$\varepsilon = \frac{\beta}{4\tan(\theta)} \tag{7}$$

Where (ε) is the microstrain, (β) is the FWHM, (θ) is half the diffraction angle position. AFM (Mountains SPIP expert 8.2.9621) device was also required for the prepared film topographical studies including surface roughness.

3. RESULTS AND DISCUSSION

The optical properties of the prepared film including the band gaps estimations for both direct and indirect allowed transitions, absorbance, and PL analyses are illustrated in Figure 2 a-d. The absorbance of the Nb_2O_5 prepared film peaked at 208 nm referring to the intrinsic semiconductor band gap, (intrinsic metal oxides thin film absorbance peaked at the UV region of the spectrum). Despite the high absorbance of the fabricated Nb_2O_5 thin film, the direct optical band gap

estimated by Tauc's plot showed a very high value that was close to the insulator range (5.3 eV) [6]. The indirect band gap estimation provided a more reasonable value that well agreed with some previous reported works and studies[33, 35]. Photoluminescence peaks were within both the UV and the visible range of the spectrum. The UV transition may refer to the near band edge emission due to the oxygen vacancy or another type of defects. The peak at 469 nm (2.6 eV) estimated for the band gap transition of the prepared film. The other peak (674 nm) may refer to the distorted octahedral NbO_6 that is the main responsible for Nb_2O_5 formation. Broadening in the observed peaks may be related to the phonon interaction that plays an important role in determinate the band gap value of the indirect allowed transition. This gives a further justification that the obtained film possessed an indirect transition. Similar indications and very approximate obtained values are found elsewhere [63-68].

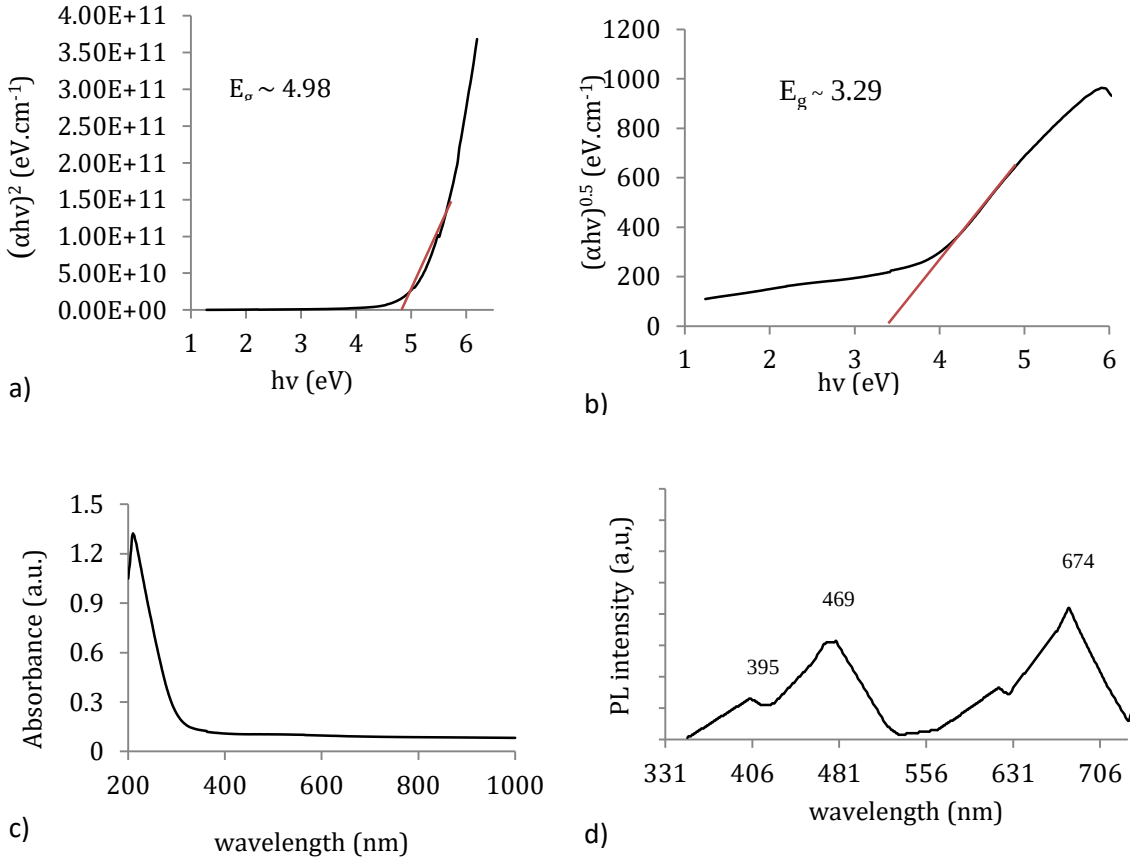

Figure 2. The obtained film optical properties including (a)direct band gap estimation. (b)indirect band gap estimation. (c) thin film absorbance. (d) PL analyses.

The XRD profile revealed that Nb_2O_5 was successfully layer-by-layer deposited forming a polycrystalline nano thin film with well-organized planes as shown in Figure 3. Interestingly, monoclinic (H-Nb_2O_5) phase was obtained by low substrate temperature and limited number of pulses. This phase is commonly obtained by higher routes temperatures in other methods[6, 67]. In addition, no other oxidation states such as NbO_2 or NbO were observed. However, orthorhombic (T-Nb_2O_5) was the predominant phase. According to JCPDS no. (09-0372) and (30-0873) as standard references, respectively. The planes that forming the crystal were oriented at (001), (402), (200), (313) and (201) with (200) was preferably oriented.

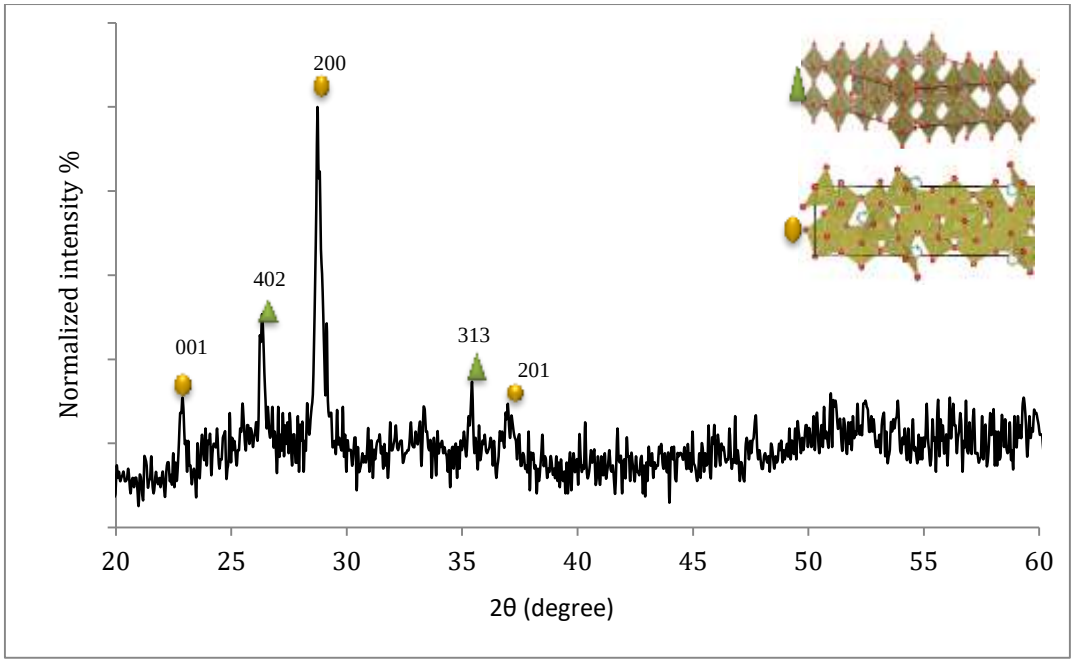

Figure 3. XRD profile of Nb_2O_5 polycrystalline thin film (T-Nb_2O_5), (H-Nb_2O_5).

Other important calculations including angles' positions, full widths at half maxima, d-spacing, dislocations, microstrain, and the obtained phases are summarized in Table 2.

Table 2 Obtained and calculated parameters from the XRD profile

2θ	d-spacing (Å)	Miller indices	D (nm)	δ (line.m^{-2})	ε	phase
22.6	3.88	001	31.24	0.00151	0.00029	T-Nb_2O_5
26.1	3.38	402	33.68	0.00088	0.00011	H-Nb_2O_5
28.8	3.10	200	23.66	0.00183	0.00038	T-Nb_2O_5
35.4	2.54	313	41.36	0.00058	0.00026	H-Nb_2O_5
36.9	2.42	201	17.12	0.00341	0.00066	T-Nb_2O_5

The most intense peak positioned at 28.8° showed a very well agreement with the standard Nb_2O_5 planes. That indicates for the importance of choosing the laser wavelength of a specific photon to interact with the electronic states of the target material. Temperature elevation as a result of electronic coupling causes the ejection of an amount that forms the plume to be deposited with the same stoichiometric elements on a substrate within a vacuum environment[68]. A careful ablation of a regularly rotated target assisted to form a well stacked deposited material on the substrate. The uniform stacking of the fabricated film layers led to build an organized crystal planes with desirable features including lower FWHM values, hence lower dislocation densities (larger crystallites' size) and well matched d-spacing parameter with JCPDS (09-0372) and (30-0873) as in Figure 4. Standard values indicating that atomic planes' formed lattice were perfectly built by PLD technique. In addition, a lower exposure to microstrains and external strains that provide unique structural, optical and topographical features for a vast range of applications. This is due to the fact that the Nb_2O_5 target was regularly rotated during the deposition process. This is one of the unique features that PLD technique possesses among other techniques. Target regular rotation assists the layer-by-layer thin film formation, thus well stacked layers with low mechanical defects such as microstrain, stress, and dislocation densities.

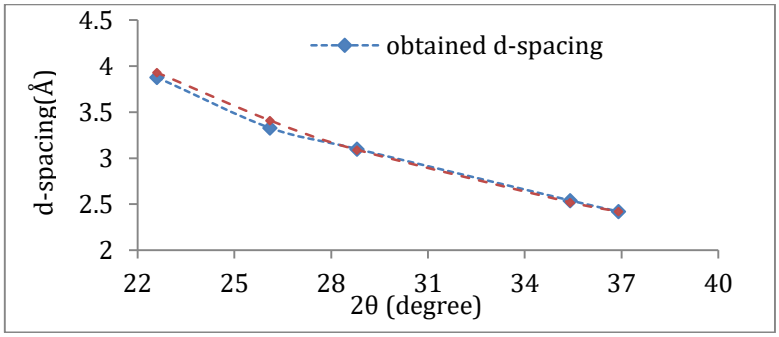

Figure 4. D-spacing of the obtained planes' lattice as compared with the standard d-spacing.

The substrate temperature is another important factor for controlling and predicting the obtained phase. The substrate temperature (350 ºC) contributed in the properties of the obtained film. Suitable substrate temperature induces the adhesion of the ejected material on the substrate, hence it greatly impacts on the final properties of the resulted thin film.

Topographical investigation of the prepared Nb_2O_5 provided some indications about the impact of the fundamental Nd:YAG laser wavelength. The thickness of the obtained thin film impacts the absorption coefficient (as in eq.2), therefore influencing the obtained band gap value. In nonmetric scale, thickness of 84.14 is reasonable with the selected number of laser shots (200 pulses) that ablated the target material. The degree of the surface roughness is one of the limitations in most applications including the fabrication of detectors (rough surface is required) and in other applications. Deposited Nb_2O_5 thin film topographical images and details are shown in Figure a-c with the related histogram.

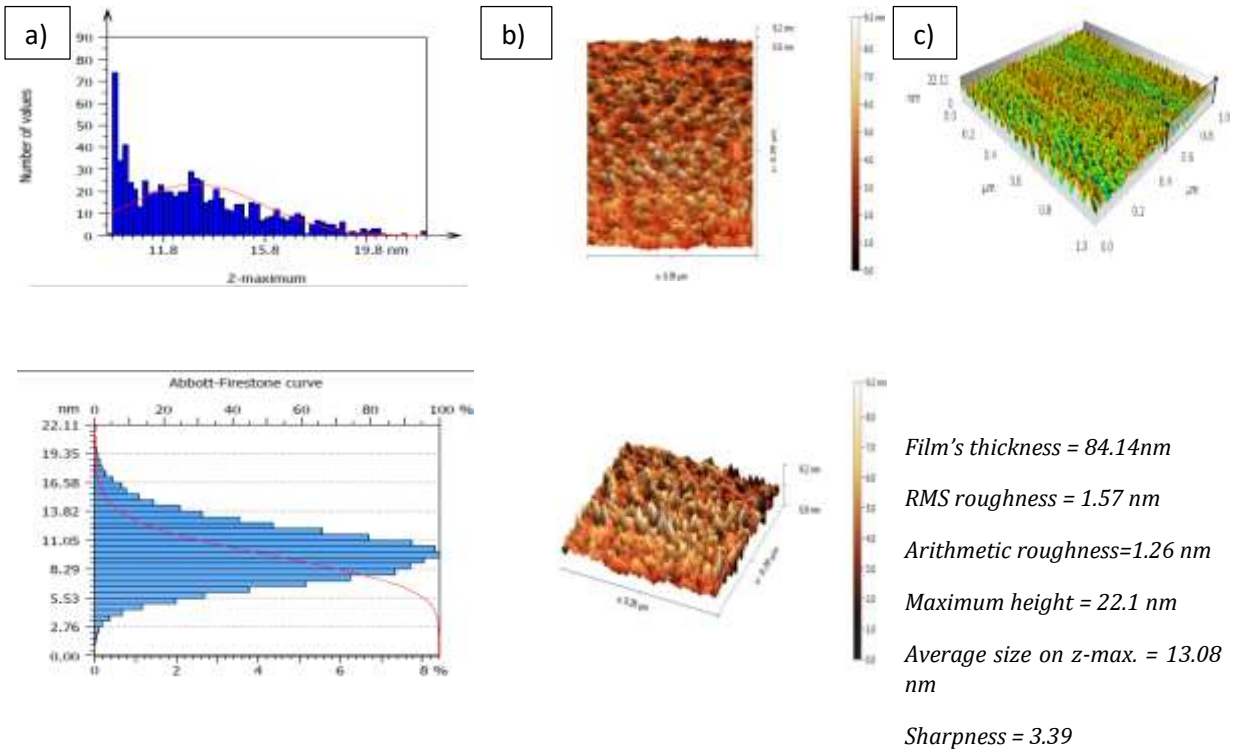

Figure 5. Thin film (a)histogram and Abbott-Firestone particles' distribution. (b) surface topography. (c) deposited plane and topographic data.

Particles' size obtained by AFM showed lower values than crystallites size calculated by XRD profile due to that AFM topographical images and analyses provide all the distributed particles on the surface top view section, while in XRD profile the calculated crystallites' size are in general related to the obtained planes of the crystal. Generally, the particle size, hence, the grain size), impacts the optical band gap value in the following manner[69-71]:

$$\Delta E = \left(\frac{h}{2me^*}\right)\frac{\pi^2}{d^2} \quad (8)$$

The equation parameters are constants including Planck's constant (h), the reduced electron mass (me*) except for (ΔE) and (d). The shifting of nanostructured semiconductor band gap (ΔE) with respect to the bulk value (3.4 eV) is inversely proportional with the particle radius. Therefore, larger particles' size induces lower microstrain, lower stress, well-matched d-spacing with the ideal lattice and lower band gap value. The sharpness value exceeded (3) revealed that height distribution is in a spiked manner. It was indicated that the growth of the grain began at substrate temperature equals to (20%) of the melting point of the material. It is also impacted by the utilized deposition technique[72]. That justifies the selected substrate temperature at 350 ºC, among other parameters, was well suited with the obtained results.

The surface morphology and the EDX analyses of the obtained Nb_2O_5 thin film are shown in Figure 6 a-b. FE-SEM image shows Nb_2O_5 nano particles that are small and spherical. In addition, most of these particles are organized in flower-like structures that are well-distributed and organized. On the other hand, some large particulates are noticeable that are normally and commonly formed when synthesizing thin films via pulsed laser technique. These particulates are generally formed as a result of the interaction of the laser photon and the target material. Physically, pulsed laser with long pulse duration (ns range) can interact with both vibrational and electronic states of the target material when it hits the target surface. That interaction can induce a localized thermal impact that elevates the irradiated volume temperature. Vaporization process is consequently occurred and the formed plasma contains different species of ions, atoms, and molecules. The selected laser energy per pulse also influences the ablation mechanism as higher energy per pulse can lead to a higher localized temperature, hence more material is evaporated and ejected [72].

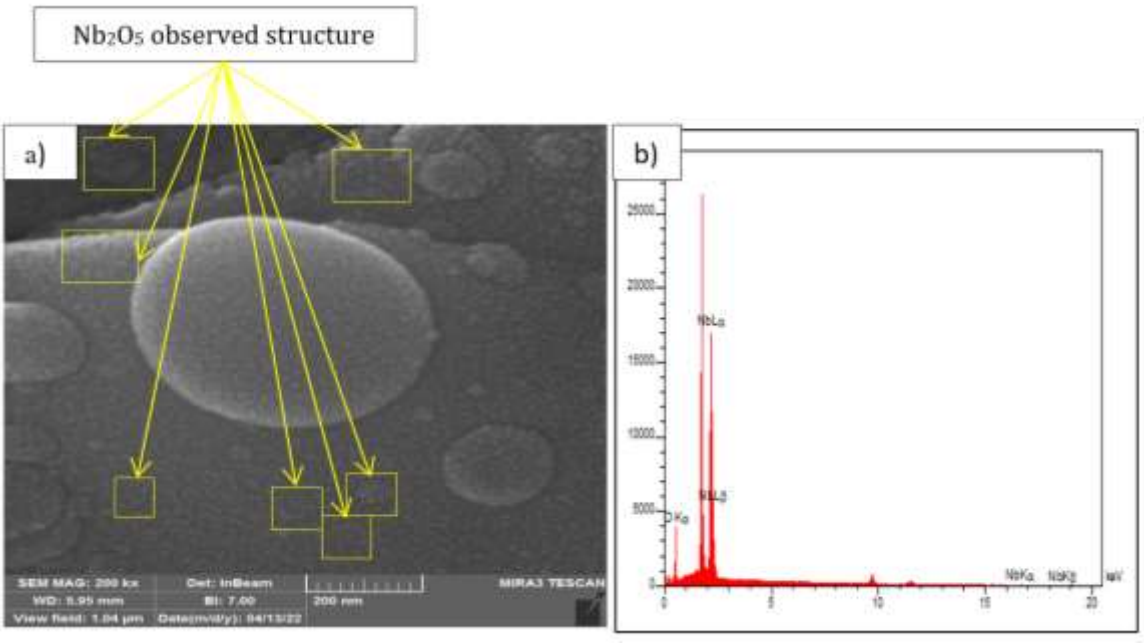

Figure 6. Nb_2O_5 prepared thin film. (a) surface morphology. (b) EDX elemental composition.

If the target material has a high coefficient of thermal expansion (temperature distribution over a wide zone) and a high melting point, then the incident photon in a ns range is unable to cause a rapid ablation. That leads to more induced thermal shockwaves, thus large solid particulates are exfoliated and observed on the substrate surface when scanned by SEM or FE-SEM.

The EDX analysis provides the elemental compositions and the purity of the formed Nb_2O_5 thin film. The results show the existence of both elements niobium (Nb) and oxygen (O) without any other elements which indicates for the high purity of the produced thin film. The elemental weights are summarized in Table 3.

Table 3 Nb_2O_5 thin film elemental weights analyzed by EDX

Nb wt.%	O wt.%	Nb/O
62.08	38.42	1.61

The high purity of the obtained Nb_2O_5 thin film prepared via pulsed laser deposition (PLD) method was due to the fact that in PLD technique, a high stoichiometry of the ablated material is produced. As the deposition process was performed in a vacuum environment and the laser source was outside the vacuum chamber, the ablated pure Nb_2O_5 target was well-transferred to the substrate as a result of no atmospheric species or contaminants that may interact with plasma plume formed by the ablation process. As the substrate was heated to 350 °C, it was sufficient for adhesion process of the arrived species from the plasma plume.

4. CONCLUSION

Under the framework of the PLD technique, Nb_2O_5 thin film was successfully obtained by Q-switched fundamental Nd:YAG pulsed laser with moderate energy 657 mJ, 200 pulses and ºC 350 selected parameters. The indirect band gap estimated by Tauc's plot was about 3.2 nm, Polycrystalline structures included Orthorhombic (T-Nb_2O_5) as well as (H-Nb_2O_5) were formed with relatively well-defined diffraction peaks. The d-spacing was very well matched with the standard value of the Nb_2O_5 indicating a high purity of the nano powder pressed in a disk-like shape target. In addition, IR Nd:YAG pulsed laser was very suitably ablated the target material and forming a nanostructured Nb_2O_5 as a thin film. The selected moderate substrate temperature showed a good coverage of nano island like structure with surface roughness suitable for different applications revealed by AFM topographical analyses.

5. FUTURE OUTLOOK AND SUGGESTIONS

As a future prospective concerned with nanotechnology and thin film fabrication, quantum dot Nb_2O_5 nanostructures can be obtained by modifying some properties including the control on the particle size obtained, noble metal decoration and other methods. The obtained results with moderate conditions that can be performed elsewhere with low cost requirements and the encouraging observed outcomes lead us to outline few suggestions. For researchers and academics who are interested in industrial field, the obtained thin film can be utilized in super capacitors, solar cells, detectors, sensors devices and as a coating surface with a desirable absorbance depending on the application. For medical and biological field, as Nb_2O_5 is featured with its corrosion resistance, dental implants and orthopedic made materials can be enhanced by Nb_2O_5 thin film. These applications and many others of Nb_2O_5 have been studied and experienced, however; PLD technique for preparing Niobia thin films and nanostructures have not fully investigated yet. For selecting the optimal conditions, a range of laser energies, a range of substrate temperature, and a range of different number of laser shots as well as different

deposition wavelengths such as the second and third harmonic Q-switched Nd:YAG laser can all be investigated to produce the best Nb_2O_5 thin films with a high quality by the simple, low cost, and fast method of the pulsed laser deposition.

REFERENCES

[1] Shafeeq, S.R, AbdulRazzaq, M.J., Salim, E.T., Wahid, M.H.A., 2022. Key Engineering Materials. 911, 89-95.

[2] Gómez, C., D., Rodríguez-Páez, J., E., 2018. Process. Appl. Ceram. 12 (No.3), 218–229, doi: 10.2298/PAC1803218G.

[3] Fakhri, M.A, Salim, E.T., Abdulwahhab, A.W., Hashim, U., Minshid, M.A, Salim, Zaid T., 2019. Surface Review and Letters. 26 (No.10), 1950068.

[4] Zhao,Y. Zhou, X., Ye, L. Chi Edman Tsang, S, 2012. Nano Rev. 3 (No.1), 17631, doi: 10.3402/nano.v3i0.17631.

[5] Fakhri, M.A., Abdulwahhab, A.W., Dawood, M.A., Raheema, A.Q., Numan, N.H., Khalid, F.G., ..., Salim, E.T., 2018. International Journal of Nanoelectronics and Materials. 11 (Special Issue BOND21), 103-108.

[6] Rani, R., A., Zoolfakar A., S., O'Mullane, A., P., Austin, M., W., Kalantar-Zadeh,K., 2014. J. Mater. Chem. A. 2 (No.38), 15683–15703, doi: 10.1039/c4ta02561j.

[7] Abood, M.K., Salim, E.T., Saimon, J.A., Hadi, A.A., 2021. International Journal of Nanoelectronics and Materials. 14 (Issue 3), 259-268.

[8] Qadir, M., Lin, J., Biesiekierski, A. Li, Y., Wen, C., 2020. ACS Appl. Mater. Interfaces. 12 (No.5), 6776–6787.

[9] Fakhri, M.A, Salim, E.T., Wahid, M.H.A., Abdulwahhab, A.W., Salim, Z.T., Hashim, U., 2019. Journal of Physics and Chemistry of Solids. 131, 180-188.

[10] Abood, M.K., Salim, Saimon, J.A., 2019. Journal of Ovonic Research. 15 (Issue 2), 109 – 115.

[11] Sayama, K. Sugihara, H. Arakawa, H., 1998. Chem. Mater. 10 (No.12), 3825–3832.

[12] Ismail, R.A., Salim, E.T., Halbos, H.T., 2021. Optik. 245, 167778.

[13] Fakhri, M.A., Khalid, F.G., Salim, E.T., 2021. Journal of Physics: Conference Series. 1795 (Issue 1), 012063

[14] Habibi, M., H., Mokhtari, R., 2012. J. Inorg. anHabibi, Mohammad Hossein Mokhtari, Rezad Organomet. Polym. Mater. 22, (No.1), 158–165.

[15] Hattab, F., Fakhry, M., 2012. First National Conference for Engineering Sciences (FNCES 2012). DOI: 10.1109/NCES.2012.6740474.

[16] Yao, D., D., Rani, R., A., O'Mullane, A., P., Kalantar-zadeh, K., Ou, J. Z., 2014. J. Phys. Chem. C. 118 (No.1), 476–481.

[17] Salim, E.T., Ismail, R.A., Fakhri, M.A, Rasheed, B.G., Z.T., Hashim, 2019. Iranian Journal of Science and Technology, Transactions A: Science. 43 (Issue 3), 1337–1343.

[18] Salim, E., T., Ismail, R. A. Halbos, H.,T., 2019. Mater. Res. Express. 6 (No.11), 116429.

[19] Jurn, Y.N., Malek, F., Mahmood, S.A., Liu, W.-W., Fakhri, M.A., Salih, M.H., 2016. Key Engineering Materials. 701, 57-66.

[20] Coşkun , Ö., D., Demirela, S, 2013. Appl. Surf. Sci. 277, 35–39.

[21] Salim, E.T., Ismail, R.A., Halbos, H.T., 2020. Appl. Phys. A. 126, 891.

[22] Blanquart ,T., 2012. Chem. Mater. 24 (No.6), 975–980.

[23] Salim, E.T., Saimon, J.A., Abood, M.K., Fakhri, M.A, 2020. Optical and Quantum Electronics. 52 (Issue 10), 463.

[24] Emeka, N., C., Imoisili, P., E., Jen, T.,-C., 2020. Coatings. 10 (No.12), 1246.

[25] Fakhri, M.A., Al-Douri, Y., Hashim, U., 2016. IEEE Photonics Journal. 8 (Issue 2), 4500410.

[26] Norton, D., R., 2007. Appl. Growth Funct. Mater.

[27] Asady, H., Salim, E.T., Ismail, R.A., 2020. AIP Conference Proceedings. 2213 (Issue 1), 020183.

[28] Mitra, A.. K., Cholkar, K. Mandal, A. Emerging Nanotechnologies for Diagnostics, Drug Delivery and Medical Devices, 2017.

[29] Mahdi, R.O., Fakhri, M.A., Salim, E.T., 2020. Materials Science Forum. 1002, 211-220.

[30] Al-Douri, Y., Fakhri, M.A., Bouhemadou, A., Khenata, R., Ameri, M., 2018. Materials Chemistry and Physics. 203, 243-248.
[31] Dai, Q., Chen, J., Lu, L., Tang, J. Wang, W., 2013. Appl. Phys. Lett. 102 (No. 20), 203904.
[32] Agool, I.R., Salim, E.T., Muhsien, M.A., 2011. International Journal of Modern Physics B. 25 (Issue 8), 1081-1089.
[33] Aubret, A., 2016. ACS Appl. Mater. Interfaces. 8 (No.34), 22361–22368.
[34] Ismail, R.A., Rasheed, B.G., Salm, E.T., Al-Hadethy, M. 2007. Journal of Materials Science: Materials in Electronics.18 (Issue 4), 397-400.
[35] Er, A., O., Elsayed-Ali, H., E., 2011. Appl. Surf. Sci. 257 (No.18), 8078–8084.
[36] Al-Douri, Y., Fakhri, M.A., Badi, N., Voon, C.H., 2018. Optik. 156, 886-890.
[37] Fu, Z., Kong, J., Qin, Q., 1999. J. Electrochem. Soc. 146 (No.10), 3914.
[38] Fakhri, M.A., Hashim, U., Salim, E.T., Salim, Z.T., 2016. Journal of Materials Science: Materials in Electronics. 27 (Issue 12), 13105-13112.
[39] Ghosh, R., 2011. ACS Appl. Mater. Interfaces. 3 (No.10), 3929–3935.
[40] Tauc, J., Menth, A., 1972. States in the gap, J. Non. Cryst. Solids. 8, 569–585.
[41] Asady, H. Salim, E.,T., Ismail, R.,A., 2020. AIP Conference Proceedings. 2213 (No.1), 20183 .
[42] Jurn, Y.N., Malek, F., Mahmood, S.A., Liu, W.-W., Gbashi, E.K., Fakhri, M.A., 2016. ARPN Journal of Engineering and Applied Sciences. 11 (Issue 8), 5108-5113.
[43] Ismail, R.A. Salim, E.T., Hamoudi, W.K., 2013. Materials Science and Engineering C. 33 (Issue 1), 47-52.
[44] Salim, E.T., Fakhri, M.A., Ismail, R.A., Abdulwahhab, A.W., Salim, Z.T., Munshid, M.A., Hashim, U., 2019. Super lattices and Microstructures. 128, 67-75.
[45] Fakhri, M.A., Al-Douri, Y., Bouhemadou, A., Ameri, M., 2017. Journal of Optical Communications. 39 (Issue 3), 297-306.
[46] Naayi, S.A., Hassan, A.I., Salim, E.T., 2018. International Journal of Nanoelectronics and Materials. 11 (Special Issue BOND21), 1-6.
[47] Hassen, H.H., Salim, E.T., Taha, J.M., Mahdi, R.O., Numan, N.H., Khalid, F.G., Fakhri, M.A., 2018. International Journal of Nanoelectronics and Materials. 11 (Special Issue BOND21), 65-72.
[48] Mohammed, D.A., Kadhim, A., Fakhri, M.A., 2018. AIP Conference Proceedings. 2045 (Issue 1), . 020014.
[49] Langenbeck, P., 1970. Appl. Opt. 9 (No.9), 2053–2058.
[50] Salim, E.T., 2013. Surface Review and Letters. 20 (Issue 05), 1350046.
[51] Fakhri, M.A., Al-Douri, Y., Salim, E.T., Hashim, U., Yusof, Y., Choo, E.B., Salim, Z.T., Jurn, Y.N., 2016. ARPN Journal of Engineering and Applied Sciences. 11 (Issue 8), 4974-4978.
[52] Fakhri, M.A., Numan, N.H., Mohammed, Q.Q., Abdulla, M.S., Hassan, O.S., Abduljabar, S.A., Ahmed, A.A., 2018. International Journal of Nanoelectronics and Materials. 11 (Special Issue BOND21), 109-114.
[53] Hassan, M.A.M., Al-Kadhemy, M.F.H., Salem, E.T., 2015. Journal of Nanoelectronics and Materials. 8 (Issue 2), 69-82.
[54] Fakhri, M.A., Al-Douri, Y., Salim, E.T., Hashim, U., Yusof, Y., Choo, E.B., Salim, Z.T., Jurn, Y.N., 2016. ARPN Journal of Engineering and Applied Sciences. 11 (Issue 8), 4974-4978.
[55] Hassan, M.M., Fakhri, M.A., Adnan, S.A.M, 2018. IOP Conf. Series: Materials Science and Engineering. 454 (Issue 1), 012172.
[56] Muhsien, M.A., Salem, E.T., Agool I.R., Hamdan, H.H., 2014. Appl. Nanoscience. 4, 719–732.
[57] Fakhri, M.A., Al-Douri, Y., Hashim, U., Salim, E.T., Prakash, D., Verma, K.D., 2015. Applied Physics B: Lasers and Optics. 121 (Issue 1), 107-116.
[58] Badr, B.A., Numan, N.H., Khalid, F.G., Fakhri, M.A., Abdulwahhab, A.W., 2019. Journal of Ovonic Research. 15 (Issue 1), 53-59.
[59] Hassan, M.A.M., Al-Kadhemy, M.F.H., Salem, E.T., 2015. Journal of Nanoelectronics and Materials. 8 (Issue 2), 69-82.
[60] Salim, E.T., Al-Wazny, M.S., Fakhri, M.A., 2013. Modern Physics Letters B. 27 (Issue 16), 1350122.
[61] Dawood, M.A., Fakhri, M.A., Khalid, F.G., Hassan, O.S., Abdulla, M.S., Ahmed, A.A., Abduljabar, S.A., 2018. IOP Conference Series: Materials Science and Engineering. 454 (Issue 1), 012161.

[62] Abdul Muhsien, M.M. Salim, E.T., Al-Douri, Y., Sale, A.F., Agool, I.R., 2015. Applied Physics A. 20 (Issue 2), 725-730.
[63] Usha, N., Sivakumar, R., Sanjeeviraja, C., Arivanandhan, M., 2015. Opt. J. Light Electron Opt. 126 (No.19), 1945–1950.
[64] Boruah, B., Gupta, R., Modak, J., M., Madras, G., 2019. Nanoscale Adv. 1 (No.7), 2748–2760.
[65] Agrahari, V., Mathpal, M.,C., Kumar, M., Agarwal, A., 2015. J. Alloys Compd. 622, 48–53.
[66] Ko, E ., I., Weissman, J., G., 1990. Catal. Today. 8 (No.1), 27–36.
[67] Norton, D., R., 2007. Thin Film. Appl. Growth Funct. Mater. 1.
[68] Thareja, R., K., Shukla, S., 2007. Appl. Surf. Sci. 253 (No.22), 8889–8895.
[69] Thompson, C., V, 1990. Grain growth in thin films, Annu. Rev. Mater. Sci. 20 (No.1), 245–268.
[70] Hassan, N.K., Fakhri, M.A., Salim, E.T., 2022. Engineering and Technology Journal. 40 (Issue 2), 422-427.
[71] Abdul Amir, H.A.A., Fakhri, M.A., Alwahib, A.A., 2022. Engineering and Technology Journal. 40 (Issue 2), 404-411.
[72] L.-C. Lin and L. C. Chen, 1994. Particulates Generated by pulsed Laser Ablation, Pulsed Laser Depos. Thin Film, 167–198.